Transfer Learning Gaussian Anomaly Detection by Fine-tuning Representations

Oliver Rippel[1][a], Arnav Chavan[2], Chucai Lei[1], and Dorit Merhof[1][b]
[1]*Institute of Imaging & Computer Vision, RWTH Aachen University, Aachen, Germany*
[2]*Indian Institute of Technology, ISM Dhanbad, India*
oliver.rippel@lfb.rwth-aachen.de

Keywords: Anomaly Detection, Anomaly Segmentation, Transfer Learning, PDF Estimation, Visual Inspection

Abstract: Current state-of-the-art anomaly detection (AD) methods exploit the powerful representations yielded by large-scale ImageNet training. However, catastrophic forgetting prevents the successful fine-tuning of pre-trained representations on new datasets in the semi-supervised setting, and representations are therefore commonly fixed. In our work, we propose a new method to overcome catastrophic forgetting and thus successfully fine-tune pre-trained representations for AD in the transfer learning setting. Specifically, we induce a multivariate Gaussian distribution for the normal class based on the linkage between generative and discriminative modeling, and use the Mahalanobis distance of normal images to the estimated distribution as training objective. We additionally propose to use augmentations commonly employed for vicinal risk minimization in a validation scheme to detect onset of catastrophic forgetting. Extensive evaluations on the public MVTec dataset reveal that a new state of the art is achieved by our method in the AD task while simultaneously achieving anomaly segmentation performance comparable to prior state of the art. Further, ablation studies demonstrate the importance of the induced Gaussian distribution as well as the robustness of the proposed fine-tuning scheme with respect to the choice of augmentations.

1 INTRODUCTION

Anomaly detection (AD) in images is concerned with finding images that deviate from a prior-defined concept of normality, and poses a fundamental computer vision problem with application domains ranging from industrial quality control (Bergmann et al., 2021) to medical image analysis (Schlegl et al., 2019). Extending AD, anomaly segmentation (AS) tries to identify the visual patterns inside anomalous images that constitute the anomaly. In general, AD/AS tasks are defined by the following two characteristics[1]:

1. Anomalies are rare events, i.e. their prevalence in the application domain is low.
2. There exists limited knowledge about the anomaly distribution, i.e. it is ill-defined.

Together, these characteristics result in AD/AS datasets that are heavily imbalanced, often containing only few anomalies for model verification and testing.

As a consequence, AD/AS algorithms focus on the semi-supervised setting, where exclusively normal data is used to establish a model of normality (Bergmann et al., 2021; Schlegl et al., 2019; Ruff et al., 2018). Since learning discriminative representations from scratch is difficult (Rippel et al., 2021c), state-of-the-art methods leverage representation gained by training on ImageNet (Deng et al., 2009) as the basis for AD/AS (Rippel et al., 2021b; Defard et al., 2020; Andrews et al., 2016; Bergmann et al., 2020; Cohen and Hoshen, 2020; Christiansen et al., 2016; Perera and Patel, 2019; Li et al., 2021).

Fine-tuning these representations on the dataset at hand now offers the potential of additional performance improvements. However, fine-tuning is hindered by catastrophic forgetting, which is defined as the loss of discriminative features initially present in the model in context of AD (Deecke et al., 2021). In fact, fine-tuning is so difficult that it is simply foregone in the majority of AD/AS approaches (refer also Section 2.1). While methods have been proposed to tackle catastrophic forgetting (Reiss et al., 2021; Deecke et al., 2020; Perera and Patel, 2019; Liznerski et al., 2021; Ruff et al., 2020; Deecke

[a] https://orcid.org/0000-0002-4556-5094
[b] https://orcid.org/0000-0002-1672-2185

[1]For a general, exhaustive overview of AD we refer the reader to (Ruff et al., 2021).

et al., 2021), they currently ignore the feature correlations inherent to the pre-trained networks (refer Figure 1, (Rodríguez et al., 2017; Ayinde et al., 2019)). Moreover, many of the aforementioned methods employ synthetic anomalies as surrogates for the true anomaly distribution to generate a supervised loss, a concept called outlier exposure (OE) (refer Figure 1) (Hendrycks et al., 2019). While performance gains have been reported here, a significant dataset bias is also induced by OE (Ye et al., 2021).

Our contributions are as follows:

- Based on findings from (Lee et al., 2018) and (Rippel et al., 2021c), we induce a multivariate Gaussian for the normal data distribution in the transfer learning setting, incorporating the feature correlations inherent to the pre-trained network. We thus propose to fine-tune the pre-trained model by minimizing the Mahalanobis distance (Mahalanobis, 1936) to the estimated Gaussian distribution using normal data only, and forego OE to avoid incorporating an additional dataset bias. We furthermore show how the proposed objective relates to and extends the prior-used optimization functions.
- We propose an early stopping criterion based on data augmentations commonly used in semi-supervised learning for vicinal risk minimization (VRM) (Chapelle et al., 2001; Hendrycks et al., 2020) to detect onset of catastrophic forgetting.
- We demonstrate the effectiveness of both proposals using the public MVTec dataset (Bergmann et al., 2021), and perform extensive ablation studies to investigate the sensitivity of our approach with respect to the chosen augmentation schemes.

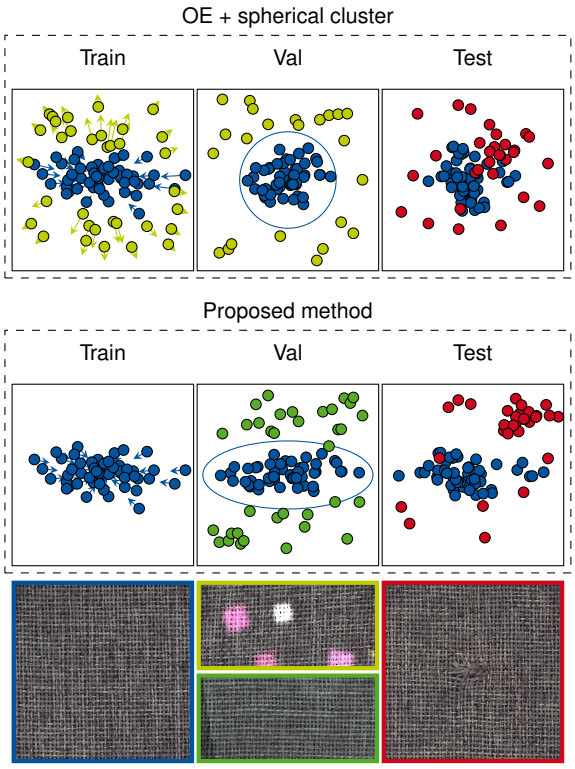

Figure 1: Comparison of the proposed method and related fine-tuning approaches. Anomalies (shown in red) are often subtle, and state-of-the-art methods use either them or synthetic anomalies (shown in yellow) for OE. However, doing so introduces a significant bias (Ye et al., 2021). Moreover, state-of-the-art fine-tuning methods ignore the feature correlations inherent to the pre-trained network (Rodríguez et al., 2017; Ayinde et al., 2019). In the proposed method, these correlations are taken into account by means of the Gaussian assumption. Furthermore, we argue that augmentations used for VRM (shown in green) are well-suited for detecting the onset of catastrophic forgetting, and can thus be used to validate semi-supervised training that uses normal data only (shown in blue). Thereby, the bias induced by OE is reduced/circumvented. A dot in the scatter plot corresponds to a complete image.

2 RELATED WORK

Features generated by large-scale dataset training (e.g. ImageNet) are commonly employed in literature to achieve AD/AS on new tasks in a transfer learning setting.

2.1 Fixed representations

The representations of the pre-trained network are commonly fixed to prevent catastrophic forgetting. To nevertheless improve AD/AS performance even with fixed representations, Bergmann et al. (Bergmann et al., 2020) employ a two-stage knowledge distillation framework to achieve AD and AS in a transfer learning setting. Here, they directly regress the intermediate representations of a ResNet18 (He et al., 2016) pre-trained on ImageNet. Furthermore, Rudolph et al. (Rudolph et al., 2021) fit an unconstrained probability distribution by means of Normalizing Flows (Rezende and Mohamed, 2015) to the nominal class.

Moreover, features from pre-trained networks are also used as the basis for classical AD methods. For example, Andrews et al. (Andrews et al., 2016) fit a discriminative one-class support vector machine (SVM) (Schölkopf et al., 2001) to features extracted from intermediate layers of a VGG (Simonyan and Zisserman, 2015) network. Furthermore, k-NN has also been used to realize AD/AS on pre-trained features (Cohen and Hoshen, 2020). Last, generative al-

gorithms such as Gaussian AD (Christiansen et al., 2016; Sabokrou et al., 2018; Defard et al., 2020; Rippel et al., 2021c) are also commonly employed.

2.2 Fine-tuning representations

Even though it offers potential benefits, fine-tuning approaches are limited by onset of catastrophic forgetting. In contrast to the typical continual learning scheme, catastrophic forgetting in AD/AS is incurred by the unavailability of anomalous data. As a consequence, discriminative feature combinations initially present in the pre-trained network are lost during fine-tuning, since they are most likely absent/missing in the normal data (Tax and Müller, 2003; Rippel et al., 2021c). Ultimately this leads to a reduced AD/AS performance.

Due to the absence of anomalies, fine-tuning approaches base their learning objective on the *concentration* assumption instead, i.e. they try to find a compact description of the normal class in high-dimensional representations. The most commonly used optimization formulation for this is the Deep support vector data description (SVDD) objective (Ruff et al., 2018), defined as

$$\min_{\mathcal{W}} \frac{1}{n}\sum_{i=1}^{n}\|\Phi(\mathbf{x}_i;\mathcal{W})-\mathbf{c}\|_1+\frac{\lambda}{2}\sum_{l=1}^{L}\|\mathbf{W}^l\|_F^2. \qquad (1)$$

Here, $\Phi : \mathbb{R}^{C\times H\times W} \rightarrow \mathbb{R}^D$ is a neural network parametrized by its weights $\mathcal{W} = \{\mathbf{W}^1, ..., \mathbf{W}^L\}$, and a hypersphere is minimized around the cluster center $\mathbf{c}$ subject to L_2 weight regularization, with $\|\cdot\|_F$ denoting the Frobenius norm.

To now overcome catastrophic forgetting, three main procedures have been proposed in literature: (I) Perera & Patel (Perera and Patel, 2019) jointly optimize Equation 1 together with the original task to ensure that the original feature discriminativeness does not deteriorate. Specifically, they use the arithmetic mean as $\mathbf{c}$ and L_2 norm over the L_1 norm in Equation 1, and perform joint optimization with ImageNet-1k training. Joint optimization, however, requires access to the original dataset, which may not always be feasible. (II) Reiss et al. (Reiss et al., 2021) propose to make use of elastic weight consolidation (EWC)(Kirkpatrick et al., 2017), a technique proposed in continual learning, to overcome catastrophic forgetting. This method, however, also requires access to the original dataset, which may again not always be feasible. (III) Deecke et al. (Deecke et al., 2021) propose to make use of L_2 regularization with respect to the initial, pre-trained weights, arguing that only subtle feature adaptations should be necessary when fine-tuning. Alternatively, they also propose to learn only a modulation of frozen features by means of newly introduced, residual adaptation layers, instead of tuning them directly.

All the aforementioned techniques can be applied in combination with OE (Hendrycks et al., 2019). Here, either synthetic anomalies or datasets disjoint to the target domain are used as surrogate anomalies to facilitate training of supervised, discriminative models. Ruff et al. (Ruff et al., 2020) formulate a hypersphere classifier (HSC) to incorporate OE to the Deep SVDD objective. Specifically, they optimize

$$\begin{aligned}\min_{\mathcal{W}} \frac{1}{n}\sum_{i=1}^{n} & y_i\|\Phi(\mathbf{x}_i;\mathcal{W})\|^2 \\ & -(1-y_i)\log\left(1-\exp(-\|\Phi(\mathbf{x}_i;\mathcal{W})\|^2\right),\end{aligned} \qquad (2)$$

where y_i denotes whether a sample is either normal ($y_i = 1$) or anomalous ($y_i = 0$). While generalization to anomalies unseen during training has been demonstrated for OE (Hendrycks et al., 2019), a bias is undoubtedly introduced by this method. Specifically, Ye et al. (Ye et al., 2021) show that labeled anomalies differing subtly from the normal class have a large impact in OE, possibly degrading performance on unseen anomaly types that are also similar to the normal class. They further show that empirical gains can only be guaranteed when anomalies are used for OE that differ strongly from the normal class instead.

Nevertheless, gains have been reported by approaches that incorporate OE, such as CutPaste (Li et al., 2021) or fully convolutional data descriptor (FCDD) (Liznerski et al., 2021). Here, CutPaste follows a two-stage procedure, i.e. fine-tuning a supervised classifier by means of OE with carefully crafted, synthetic anomalies followed by Gaussian AD as proposed in (Rippel et al., 2021c). FCDD applies the HSC objective to spatial feature maps, i.e. intermediate representations of a pre-trained network that still possess spatial dimensions, to fine-tune the network directly. Similar to CutPaste, they also use carefully crafted, synthetic anomalies for OE.

Out of all related works, only FCDD and CutPaste evaluate performance on a dataset where normal and anomalous classes differ subtly, namely the MVTec dataset (Bergmann et al., 2021).

3 TRANSFER LEARNING GAUSSIAN ANOMALY DETECTION

In our work, we propose to fine-tune the representations of pre-trained networks based on the Gaussian assumption. A motivation behind the seemingly

overly simplistic Gaussian assumption can be inferred from Lee et al. (Lee et al., 2018). Here, authors have induced a Gaussian discriminant analysis (GDA) for out-of-distribution (OOD) detection. Investigations into the unreasonable effectiveness of the Gaussian assumption by Kamoi and Kobayashi (Kamoi and Kobayashi, 2020) have revealed that feature combinations containing low variance for the normal/nominal class are ultimately those discriminative to the OOD data. Independent investigations into the same phenomenon for AD by Rippel et al. (Rippel et al., 2021c) have revealed the same finding for the transfer learning setting. However, despite its elegant simplicity and outstanding performance, the Gaussian assumption has not yet been used to fine-tune pre-trained features for AD.

The Gaussian distribution is given by

$$\varphi_{\mu,\Sigma}(\mathbf{x}) := \frac{1}{\sqrt{(2\pi)^D |\det \Sigma|}} e^{-\frac{1}{2}(\mathbf{x}-\mu)^\top \Sigma^{-1}(\mathbf{x}-\mu)}, \quad (3)$$

with D being the number of dimensions, $\mu \in \mathbb{R}^D$ being the mean vector and $\Sigma \in \mathbb{R}^{D\times D}$ being the symmetric covariance matrix of the distribution, which must be positive definite.

Under a Gaussian distribution, a distance measure between a particular point $\mathbf{x} \in \mathbb{R}^D$ and the distribution is called the Mahalanobis distance (Mahalanobis, 1936), given as

$$M(\mathbf{x}) = \sqrt{(\mathbf{x}-\mu)^\top \Sigma^{-1} (\mathbf{x}-\mu)}. \quad (4)$$

Let us compare the Mahalanobis distance (Equation 4) to the Deep SVDD objective (Equation 1). When imposing a univariate Gaussian with zero-mean and unit-variance per feature, the Mahalanobis distance reduces to the L_2 distance to the mean, recapitulating the original Deep SVDD objective with L_2 norm instead of L_1 norm. In other words, minimizing the Deep SVDD objective in conjunction with L_2 norm *implicitly assumes* that features follow independent, univariate Gaussians with zero-mean and unit-variance. This assumption, however, is in disagreement with findings in literature, where strong correlations have been observed across deep features extracted from convolutional neural networks (CNNs) (Rodríguez et al., 2017; Ayinde et al., 2019). Our induced multivariate Gaussian prior thus actually imposes a lesser inductive bias than the Deep SVDD objective, and allows for more flexible distributions. Internal experiments furthermore showed that identical performance could be achieved when decorrelating the pre-trained features by means of Cholesky decomposition prior to training them with the Deep SVDD objective.

Since others (Cohen and Hoshen, 2020; Defard et al., 2020; Liznerski et al., 2021) have demonstrated that good AS performance can be achieved by utilizing intermediate feature representations that maintain spatial dimensions, we propose to apply the Mahalanobis distance to Gaussians fitted to intermediate feature representations as well. Specifically, let $\Phi : \mathbb{R}^{C\times H\times W} \to \mathbb{R}^D$ be a CNN with its intermediate mappings denoted as $\Phi_m : \mathbb{R}^{C_{m-1}\times H_{m-1}\times W_{m-1}} \to \mathbb{R}^{C_m\times H_m\times W_m}$. Then, the Mahalanobis distance of Φ_m is a given by applying Equation 4 to each spatial element independently, yielding a matrix $\mathbf{A}_m$ of size $H_m \times W_m$. Note that we account for small local changes in image composition by modeling μ independently per location & tie Σ across locations. This has already been shown to be particularly powerful for fixed features in (Rippel et al., 2021a), and we perform an evaluation of its effectiveness in Section 4.2.1. Furthermore, we use $max(\mathbf{A})$ to give an anomaly score per level m of Φ, which is also used for optimization. Using $max(\mathbf{A})$ over $mean(\mathbf{A})$ is motivated by (Defard et al., 2020), which have shown that strong AD results can be achieved by aggregating in such a manner for fixed representations. We argue that, when fine-tuning AD, one wants to modify exactly those feature combinations that are currently most perceived to be anomalous for normal images, in order to ensure that the true data distribution fits the estimated Gaussian distribution better, and assess its effects in Section 4.2.1.

Our overall minimization objective is thus

$$\min_{\mathcal{W}} \frac{1}{n\cdot m} \sum_{i=1}^{n} \sum^{m} max(\mathbf{A}_m(\Phi(\mathbf{x}_i;\mathcal{W}))). \quad (5)$$

Note that the parameters μ_m and Σ_m of the Gaussians are not learned. Instead, we use the empirical mean μ_m and estimate Σ_m using shrinkage as proposed by Ledoit et al. (Ledoit et al., 2004), and leave them fixed afterwards. This yields a stronger bias and was shown to prevent catastrophic forgetting in prior experiments.

For AS, we propose to upsample $\mathbf{A}_m$ using bilinear interpolation similarly to (Cohen and Hoshen, 2020; Defard et al., 2020) over Gaussian interpolation. Bilinear interpolation is free of hyperparameters and thus more robust while simultaneously offering competitive results (selection of the Gaussian interpolation kernel was shown to have a strong effect on AS performance in (Liznerski et al., 2021)). After their respective upsampling, pixel-wise averaging across all heatmaps yields the overall anomaly score map.

Note that while OE could be easily integrated into our proposed approach by maximizing Equation 5 for

synthetic anomalies, we forego it to avoid the induction of an additional bias incurred by providing surrogates for the anomaly distribution (Ye et al., 2021).

3.1 Early stopping via VRM

While we forego OE, we still need to detect onset of catastrophic forgetting. To this end, we propose to approximate the compactness/discriminativeness of the learned distribution. Specifically, we argue that a good model should be able to distinguish between subtle variations of the normal data and the normal data itself as a surrogate for AD performance. We therefore sample the vicinity of the normal data distribution by employing augmentations used for VRM in semi-supervised learning schemes (refer Figure 1). Afterwards, we measure the capability of a tuned network Φ to distinguish between subtle vicinal variations and normal data by means of area under the receiver operating characteristic (ROC) curve (AUROC) as surrogate of the model's discriminativeness. We select both best model state based on this criterion and perform early stopping should AUROC no longer improve. As multiple augmentation schemes have been proposed for VRM in literature, we compare *AugMix* (Hendrycks et al., 2020) with *CutOut* (DeVries and Taylor, 2017) to investigate the dependence of early stopping on augmentation types. Additionally, we compare with *Confetti* noise, but note that this has been introduced as a surrogate for the anomaly distribution originally in (Liznerski et al., 2021).

We furthermore note that validating the model by assessing its capability to distinguish between subtle variations and normal data could introduce an additional bias. We argue however, that this bias should be less strong than when using these subtle variations for OE directly, and show this to be the case in Section 4.2.

4 EXPERIMENTS

First, we briefly introduce the dataset used for evaluating our approach as well as the employed metrics.

4.1 Dataset and Evaluation metrics

We use the public MVTec dataset (Bergmann et al., 2021) to test and compare our approach with literature. The reasons for this are two-fold: First, MVTec consists of subtle anomalies in high-resolution images as opposed to the AD tasks commonly constructed from classification datasets (e.g. one-versus-rest based on CIFAR-10 (Liznerski et al., 2021)). Therefore, MVTec is more challenging and indicative of real-world AD/AS performance. Second, MVTec provides binary segmentation masks that can be used to evaluate AS performance, which is infeasible for classification datasets. MVTec itself consists of 15 industrial product categories in total (10 object and 5 texture classes), and contains 5354 images overall.

To evaluate AD performance, we report the AUROC, a metric commonly used to evaluate binary classifiers (Ferri et al., 2011). For AS, we report the pixel-wise AUROC as well as the per-region-overlap (PRO) curve until 30% false positive rate (FPR) as proposed in (Bergmann et al., 2020). While pixel-wise AUROC represents an algorithm's capability of identifying anomalous pixels, PRO focuses more on an algorithm's performance at detecting small, locally constrained anomalies.

4.2 Anomaly Detection

We first assess whether our proposed fine-tuning approach improves AD performance.

Training & Evaluation details. We perform a 5-fold evaluation over the training set of each MVTec category, training an EfficientNet-B4 (Tan and Le, 2019) to minimize the objective given by Equation 5, and split the training dataset into 80% used for training and 20% used for validation. We choose EfficientNet based on its strong ImageNet performance (Tan and Le, 2019), as architectures with stronger ImageNet performance have been shown to yield better features for transfer learning in (Kornblith et al., 2019), which has been further confirmed for transfer learning in AD (Rippel et al., 2021c). Moreover, EfficientNet-B4s have been shown to offer a good trade-off between model complexity and AD performance (Rippel et al., 2021c). To demonstrate the general applicability of our approach, we omit the selection of best-performing feature levels, simply extracting the features from every "level" of the EfficientNet as denoted in (Tan and Le, 2019). We also train models to minimize the Deep SVDD (Equation 1) and FCDD objectives. Here, we apply our early stopping criterion to both objectives, and simultaneously use the synthetic anomalies for OE in the FCDD objective. This is done to factor out differences in model performance yielded by changing the underlying feature extractor (to the best of our knowledge, Deep SVDD and FCDD objectives have not yet been applied to EfficientNets for transfer learning AD in the fine-tuning setting). All models are trained using a batch size of 8, Adam optimizer (Kingma and Ba,

2015) and a learning rate of 1.0×10^{-6}. The small learning rate is motivated by the fact that the feature representations are already discriminative as is (refer e.g. to the fixed baseline in Table 1), and only need to be tuned slightly. Furthermore, BatchNormalization (Ioffe and Szegedy, 2015) statistics were kept frozen, as dataset sizes are too small to re-estimate them reliably. Training was stopped when validation AUROC performance did not improve for 20 epochs, and 70% of validation data was augmented and marked as anomalous. We randomly sample 10 times the length of our validation dataset for validation to better approximate overall population characteristics, and sample augmentations from all VRM-schemes with equal probability (refer also Section 4.2.1). In all experiments, we report $\mu\pm$ standard error of the mean (SEM) aggregated over the 15 MVTec categories.

Results. Analyzing results (Table 1), it can be seen that our proposed transfer learning scheme improves over the baseline (frozen features), increasing AD performance from 96.3 ± 1.1 to 97.1 ± 0.8 AUROC and setting a new state-of-the-art in AD on the public MVTec dataset. Furthermore, it can be seen that the Gaussian assumption is important, since SVDD and FCDD objectives are already outperformed by our baseline where no fine-tuning of feature representations occurs (90.5 ± 2.7 and 87.0 ± 3.6 vs. 96.3 ± 1.1). Still, it should be noted that fine-tuning using our proposed early stopping criterion improves results also here (86.7 ± 3.5 to 90.5 ± 2.7 and 87.0 ± 3.6). Comparing Deep SVDD and FCDD performances, it can be seen that worse AD performance is achieved when using the subtle variations for OE rather than just using them for model validation.

4.2.1 Ablation studies

Next, we perform ablation studies to quantify the effects of proposed early stopping procedure, parametrization of the Gaussian distribution + aggregation of spatial anomaly scores on AD performance.

Proposed early stopping procedure. We perform two different experiments to assess effects of the proposed early stopping procedure.

First, we investigate effects of early stopping itself, comparing the proposed approach to both (I) the training for a fixed number of epochs (250 specifically) and (II) the early stopping without sampling the vicinity of the normal data distribution. Here, we use the minimum loss of Equation 5 over the validation set as an early stopping criterion and omit sampling the vicinity, focussing only on how well the normal data fits the distribution.

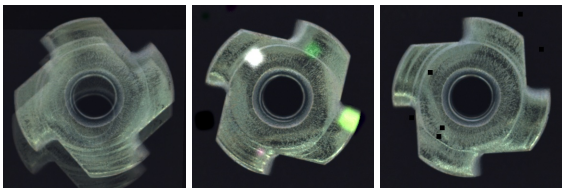

(a) (b) (c)

Figure 2: Reference synthesis results generated by (a) *AugMix*, (b) *Confetti* and (c) *CutOut* for the metal nut class.

Assessing results (Table 2), it can be seen that our proposed early stopping criterion is the only method that improves results. Furthermore, early stopping based on validation loss alone leads to worse results than training for a fixed number of epochs. Thus, validation loss alone is unable to detect onset of catastrophic forgetting. It should also be noted that manually tuning the number of fixed epochs for training could have eventually led to improved results. Such a tuning, however, would need to be performed in a dataset specific manner and is not needed by our proposed early stopping criterion.

Second, we assess the method's sensitivity with respect to the chosen VRM-type. To this end, we perform an additional ablation study, varying the severity of *AugMix* (Hendrycks et al., 2020) and investigate the suitability of *CutOut* (DeVries and Taylor, 2017) and *Confetti noise* (Liznerski et al., 2021). We sample the depth of *AugMix* uniformly from [1, 3], as further increasing the depth produced too strong variations in image appearance. We also investigate benefits yielded by combining different augmentation schemes, where the augmentation of a sample is drawn randomly from $\{AugMix, CutOut, Confetti\}$ with equal probability. A reference image for each synthesis procedure is shown in Figure 2.

Assessing results (Table 3), it can be seen that all augmentation schemes improve results over the baseline, where feature adaptation is omitted (Table 1). Furthermore, *AugMix* outperforms the other two methods slightly, and the performance is invariant to the severity of applied augmentations. Last, when jointly applying all augmentations, the same performance is reached as when applying only the best augmentation. This indicates that augmentation schemes do not affect each other negatively, and reduces the complexity of the approach: One can simply pool multiple augmentation strategies and still achieve the overall best performance.

Gaussian types & aggregation. We also investigate the effects of both different distribution types fit

Table 1: Comparison to the state of the art for AD. We report $\mu \pm$ SEM AUROC scores in percent aggregated over all MVTec categories. Note that values reported for GeoTrans and GANomaly were taken from (Fei et al., 2020), and values reported for US from (Zavrtanik et al., 2020). Abbreviations: SEM = standard error of the mean.

Approach	Feature type	Mean ↑	SEM ↓
GeoTrans (Golan and El-Yaniv, 2018)	Scratch	67.2	4.7
GANomaly (Akçay et al., 2018)	Scratch	76.1	1.6
ARNet (Fei et al., 2020)	Scratch	83.9	2.8
RIAD (Zavrtanik et al., 2020)	Scratch	91.7	1.8
US (Bergmann et al., 2020)	Scratch	87.7	2.8
SPADE (Cohen and Hoshen, 2020)	Frozen	85.5	—
Differnet (Rudolph et al., 2021)	Frozen	94.7	1.3
PaDiM (Defard et al., 2020)	Frozen	95.3	—
Patch SVDD (Yi and Yoon, 2020)	Scratch	92.1	1.7
Triplet Networks (Tayeh et al., 2020)	Scratch	94.9	1.2
CutPaste (Li et al., 2021)	Tuned	96.6	1.1
Gaussian AD (Rippel et al., 2021c)	Frozen	95.8	1.2
Gaussian fine-tune (ours)	Tuned	**97.1**	**0.8**
	Frozen	96.3	1.1
Deep SVDD	Tuned	90.5	2.7
	Frozen	86.7	3.5
FCDD	Tuned	87.0	3.6

Table 2: Effects of early stopping criterion on fine-tuning AD performance.

Method	Mean ↑	SEM ↓
Vicinity sampling via VRM	97.1	0.9
Fixed epochs	96.3	1.2
Validation loss	95.4	1.2
No Training	96.3	1.1

Table 3: Effect of VRM-type on AD performance.

Method	Mean ↑	SEM ↓
AugMix		
sev = 3	97.1	0.8
sev = 4	97.0	0.9
sev = 5	97.0	0.8
sev = 6	97.0	0.8
sev = 7	97.1	0.8
Confetti noise	96.7	1.0
CutOut	96.6	1.0
All	97.1	0.8

to the normal class and spatial aggregation of anomaly scores on AD performance. Specifically, we compare a global Gaussian distribution (shared μ and Σ across all spatial locations of a "level"), a tied Gaussian distribution (individual μ and tied Σ) as well as local Gaussian distributions (individual μ and Σ per location). Except for the parametrization of the Gaussian, training details are identical as before. For the aggregation methods, we compare mean and maximum aggregation for generation of image-level AD scores.

Table 4: Effect of different types of distribution/aggregation methods on AD performance.

Method	Mean ↑	SEM ↓
Global Gaussian		
aggregation = mean	93.7	2.3
aggregation = max	96.9	0.9
One Gaussian per location		
aggregation = mean	97.3	0.8
aggregation = max	97.3	0.8
Tied Gaussian		
aggregation = mean	93.0	2.3
aggregation = max	97.1	0.8

When assessing results (Table 4), it can be seen that maximum aggregation performs best across all methods. Furthermore, effects of max aggregation are stronger for the global as well as the tied Gaussian distribution than the local Gaussian fit per location. Overall, AD performance of the local Gaussian model is best. However, it also has the highest memory requirement, increasing the overall memory footprint of the method by a factor of 10. Notably, it also has the highest base AD performance and only negligible gains are achieved by fine-tuning. It is therefore infeasible in practice, and not regarded further.

4.3 Anomaly Segmentation

Since our approach maintains spatial resolution of anomaly scores, AS can also be achieved similarly to (Liznerski et al., 2021; Defard et al., 2020).

Training & Evaluation details. To factor out effects of pre-trained model selection on AS performance and give a fair comparison to competing fine-tuning methods, we also report AS performance of EfficientNet-B4s fine-tuned with either FCDD + OE or Deep SVDD. All other hyperparameters are same as in Section 4.2.

Results. Assessing results, it can be seen that our proposed fine-tuning scheme improves both AUROC (Table 5) and PRO (Table 6) scores. This is in contrast to Deep SVDD, where both AUROC and PRO decrease upon fine-tuning. Conversely, the FCDD objective also improves AS performance, and we achieve higher AUROC values for FCDD than reported in (Liznerski et al., 2021). Furthermore, differences across the fine-tuning objectives are much lower for AS than for AD. Compared to state-of-the-art AS methods, our method achieves similar AUROC scores, and slightly lower PRO scores.

In addition to quantitative evaluations, we also assess segmentation results qualitatively, showcasing representative results in Figure 3. Here, it can be seen that our approach performs well on low-level, textural anomalies (e.g. the "print" on the hazelnut as well as the "glue" on the leather). However, it fails to segment/capture high-level, semantic anomalies such as the "cable swap" or "scratches" ("scratches" may be similar in appearance to the background texture in context of the class wood).

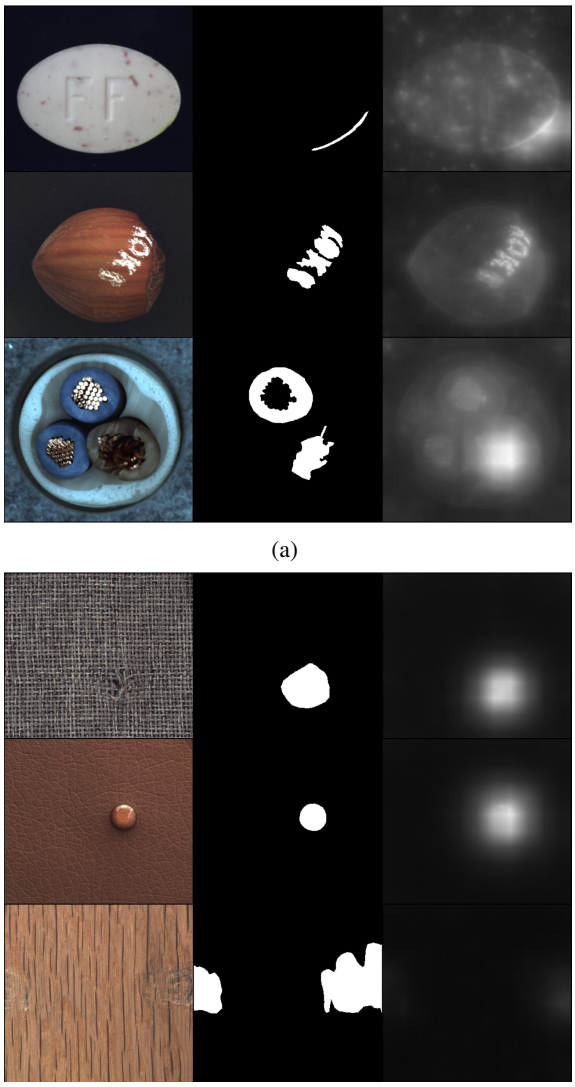

Figure 3: Representative successful segmentations as well as failure cases of our approach. We show representative successful segmentations as well as failures for three categories (a) as well as three texture (b) classes of the MVTec dataset. Left shows the input image, the middle the ground-truth segmentation mask, and the right the heatmap generated by our approach. Heatmaps are scaled such that the value range across all test images is mapped to the interval [0, 255].

5 DISCUSSION

In our work, we have proposed to fine-tune pre-trained feature representations for AD using Gaussian distributions, and motivated this by the linkage between generative and discriminative modeling shown in (Lee et al., 2018; Kamoi and Kobayashi, 2020; Rippel et al., 2021c). We have also proposed to use augmentations commonly employed for VRM to detect onset of catastrophic forgetting, avoiding the bias likely induced by sampling the anomaly distribution for OE (Ye et al., 2021).

Evaluations on the public MVTec dataset have revealed that the proposed fine-tuning based on the Gaussian assumption achieves a new state-of-the-art in AD and improves AS performance (Table 1, Table 5 and Table 6). Ablation studies demonstrated that onset of catastrophic forgetting can be reliably detected using our proposed early stopping criterion (Table 2). We have furthermore shown that the choice of augmentation scheme only has a limited influence on the detection of catastrophic forgetting. Moreover, ensembling multiple augmentation schemes yields results equal to that of the best scheme applied individ-

Table 5: AUROC scores in percent for pixel-wise segmentation. We report $\mu \pm$SEM across MVTec categories. Values reported for US were sourced from (Zavrtanik et al., 2020).

Approach	Feature type	Mean ↑	SEM ↓
CAVGA-R_u (Venkataramanan et al., 2020)	Scratch	89.0	—
RIAD (Zavrtanik et al., 2020)	Scratch	94.2	1.3
VAE-Attention (Liu et al., 2020)	Scratch	86.1	2.3
US (Bergmann et al., 2020)	Scratch	93.9	1.6
SPADE (Cohen and Hoshen, 2020)	Frozen	96.0	0.9
PaDiM (Defard et al., 2020)	Frozen	**97.5**	**0.4**
Patch SVDD (Yi and Yoon, 2020)	Scratch	95.7	0.6
FCDD (Liznerski et al., 2021)	Tuned	92.0	—
CutPaste (Li et al., 2021)	Tuned	96.0	0.8
Gaussian fine-tune (ours)	Tuned	96.5	0.8
	Frozen	96.4	0.7
Deep SVDD	Tuned	95.1	0.9
	Frozen	95.2	0.9
FCDD	Tuned	96.2	0.6

Table 6: Area under the PRO curve as defined by (Bergmann et al., 2021; Bergmann et al., 2020) up to a false positive rate of 30%. Values for state-of-the-art methods are directly taken from the corresponding sources. We report $\mu \pm$SEM values.

Approach	Feature type	Mean ↑	SEM ↓
SPADE (Cohen and Hoshen, 2020)	Frozen	91.7	1.4
PaDiM (Defard et al., 2020)	Frozen	**92.1**	**1.1**
US (Bergmann et al., 2020)	Frozen	91.4	2.0
Gaussian fine-tune (ours)	Tuned	88.7	1.7
	Frozen	88.5	1.6
Deep SVDD	Tuned	88.7	1.9
	Frozen	88.9	2.0
FCDD	Tuned	89.7	1.6

ually (Table 3). Our proposed early stopping regime should thus be transferable also to other fine-tuning approaches and can easily integrate additional augmentation schemes such as the one proposed in (Li et al., 2021).

We furthermore remarked in Section 3.1 that a bias may still be introduced even when using subtle augmentations for model validation rather than OE, but argued that this bias would most likely be lower. Results showed that Deep SVDD outperforms FCDD with respect to AD (Table 1), supporting this claim. While FCDD did outperform Deep SVDD with respect to AS, this can be attributed by the segmentation mask generated for the synthetic *Confetti* and *CutOut* augmentations, which provide additional information about anomaly localization leveraged by FCDD. Therefore, one should train FCDD without exploiting the synthetic segmentation masks in future work to fully validate our claim.

During our evaluations, we moreover found that FCDD achieves better AS than reported in (Liznerski et al., 2021). This can be in part attributed to the fact that we apply FCDD to multiple levels of the pre-trained CNN. Furthermore, we use features of an EfficientNet-B4 compared to the VGG16 used in (Liznerski et al., 2021), and network architectures with better ImageNet performance have been shown to be more suited for transfer learning in (Kornblith et al., 2019).

5.1 Limitations

While both AD and AS could be improved by fine-tuning, our approach failed to segment high-level, semantic anomalies (cf. Figure 3). High-level, semantic anomalies are undoubtedly more difficult to detect than low-level anomalies, as they require a model of normality that is defined on an abstract understanding of the underlying image domain (Ahmed and Courville, 2020; Deecke et al., 2021). Acquiring such abstract understanding has proven difficult for CNNs, as evidenced by their texture-bias (Geirhos

et al., 2019; Hermann et al., 2020). Potentially, learning these concepts could be achieved by employing the self-attention mechanism (Vaswani et al., 2017), and a lesser texture bias was observed for vision transformers (ViTs) (Dosovitskiy et al., 2021) recently (Naseer et al., 2021). Thus, one should try to apply features of ImageNet pre-trained ViTs to the AS task in future work. As an alternative, one could also try to leverage features yielded by either object detection or segmentation networks, which have been shown to generate features that maintain stronger spatial acuity (Li et al., 2019). They have furthermore been shown to improve AS performance when used as the basis for transfer learning AS (Rippel and Merhof, 2021). Moreover, we limited our evaluations to the public MVTec dataset. In future work, we will therefore revalidate our approach on additional datasets used in literature, such as CIFAR-10 (Ahmed and Courville, 2020). Last, anomalies may also occur for multimodal normal data distributions (Rippel et al., 2021d; Deecke et al., 2021), and our current fine-tuning procedure can not be applied here. Here, less constrained priors such as Gaussian mixture models or normalizing flows (Rezende and Mohamed, 2015) may be used instead.

6 CONCLUSION

In our work, we have demonstrated that fine-tuning of pre-trained feature representations for transfer learning AD is possible using a strong Gaussian prior, achieving a new state-of-the-art in AD on the public MVTec dataset. We have further shown that augmentations commonly employed for VRM can be used to detect onset of catastrophic forgetting, which typically hinders transfer learning in AD. Here, ablation studies revealed that our method is robust with respect to the chosen synthesis scheme, and that combining multiple schemes is also feasible. Together, this demonstrated the general applicability of our approach.

REFERENCES

Ahmed, F. and Courville, A. (2020). Detecting semantic anomalies. *Proceedings of the AAAI Conference on Artificial Intelligence*, 34(04):3154–3162.

Akçay, S., Atapour-Abarghouei, A., and Breckon, T. P. (2018). GANomaly: Semi-supervised anomaly detection via adversarial training. In *Asian Conference on Computer Vision*, pages 622–637. Springer.

Andrews, J., Tanay, T., Morton, E. J., and Griffin, L. D. (2016). Transfer representation-learning for anomaly detection. JMLR, Multidisciplinary Digital Publishing Institute.

Ayinde, B. O., Inanc, T., and Zurada, J. M. (2019). Regularizing deep neural networks by enhancing diversity in feature extraction. *IEEE Transactions on Neural Networks and Learning Systems*, 30(9):2650–2661.

Bergmann, P., Batzner, K., Fauser, M., Sattlegger, D., and Steger, C. (2021). The mvtec anomaly detection dataset: A comprehensive real-world dataset for unsupervised anomaly detection. *International Journal of Computer Vision*.

Bergmann, P., Fauser, M., Sattlegger, D., and Steger, C. (2020). Uninformed students: Student-teacher anomaly detection with discriminative latent embeddings. In *Proceedings of the IEEE/CVF Conference on Computer Vision and Pattern Recognition*, pages 4183–4192.

Chapelle, O., Weston, J., Bottou, L., and Vapnik, V. (2001). Vicinal risk minimization. In Leen, T., Dietterich, T., and Tresp, V., editors, *Advances in Neural Information Processing Systems*, volume 13. MIT Press.

Christiansen, P., Nielsen, L. N., Steen, K. A., Jørgensen, R. N., and Karstoft, H. (2016). Deepanomaly: Combining background subtraction and deep learning for detecting obstacles and anomalies in an agricultural field. *Sensors*, 16(11):1904.

Cohen, N. and Hoshen, Y. (2020). Sub-image anomaly detection with deep pyramid correspondences. *arXiv preprint arXiv:2005.02357*.

Deecke, L., Ruff, L., Vandermeulen, R. A., and Bilen, H. (2020). Deep anomaly detection by residual adaptation. *arXiv preprint arXiv:2010.02310*.

Deecke, L., Ruff, L., Vandermeulen, R. A., and Bilen, H. (2021). Transfer-based semantic anomaly detection. In Meila, M. and Zhang, T., editors, *Proceedings of the 38th International Conference on Machine Learning*, volume 139 of *Proceedings of Machine Learning Research*, pages 2546–2558. PMLR.

Defard, T., Setkov, A., Loesch, A., and Audigier, R. (2020). Padim: a patch distribution modeling framework for anomaly detection and localization. *arXiv preprint arXiv:2011.08785*.

Deng, J., Dong, W., Socher, R., Li, L., Li, K., and Fei-Fei, L. (2009). ImageNet: A large-scale hierarchical image database. In *2009 IEEE Conference on Computer Vision and Pattern Recognition*, pages 248–255.

DeVries, T. and Taylor, G. W. (2017). Improved regularization of convolutional neural networks with cutout. *arXiv preprint arXiv:1708.04552*.

Dosovitskiy, A., Beyer, L., Kolesnikov, A., Weissenborn, D., Zhai, X., Unterthiner, T., Dehghani, M., Minderer, M., Heigold, G., Gelly, S., Uszkoreit, J., and Houlsby, N. (2021). An image is worth 16x16 words: Transformers for image recognition at scale. In *International Conference on Learning Representations*.

Fei, Y., Huang, C., Jinkun, C., Li, M., Zhang, Y., and Lu, C. (2020). Attribute restoration framework for anomaly detection. *IEEE Transactions on Multimedia*.

Ferri, C., Hernández-Orallo, J., and Flach, P. A. (2011). A coherent interpretation of AUC as a measure of aggregated classification performance. In *Proceedings of the 28th International Conference on Machine Learning (ICML-11)*, pages 657–664.

Geirhos, R., Rubisch, P., Michaelis, C., Bethge, M., Wichmann, F. A., and Brendel, W. (2019). Imagenet-trained CNNs are biased towards texture; increasing shape bias improves accuracy and robustness. In *International Conference on Learning Representations*.

Golan, I. and El-Yaniv, R. (2018). Deep anomaly detection using geometric transformations. In *Advances in Neural Information Processing Systems*, pages 9758–9769.

He, K., Zhang, X., Ren, S., and Sun, J. (2016). Deep residual learning for image recognition. In *Proceedings of the IEEE conference on computer vision and pattern recognition*, pages 770–778.

Hendrycks, D., Mazeika, M., and Dietterich, T. (2019). Deep anomaly detection with outlier exposure. In *International Conference on Learning Representations*.

Hendrycks, D., Mu, N., Cubuk, E. D., Zoph, B., Gilmer, J., and Lakshminarayanan, B. (2020). AugMix: A simple data processing method to improve robustness and uncertainty. *Proceedings of the International Conference on Learning Representations (ICLR)*.

Hermann, K. L., Chen, T., and Kornblith, S. (2020). The origins and prevalence of texture bias in convolutional neural networks. In Larochelle, H., Ranzato, M., Hadsell, R., Balcan, M., and Lin, H., editors, *Advances in Neural Information Processing Systems 33: Annual Conference on Neural Information Processing Systems 2020, NeurIPS 2020, December 6-12, 2020, virtual*.

Ioffe, S. and Szegedy, C. (2015). Batch normalization: Accelerating deep network training by reducing internal covariate shift. In *Proceedings of the 32nd International Conference on International Conference on Machine Learning - Volume 37*, ICML'15, page 448–456, Lille, France. JMLR.org.

Kamoi, R. and Kobayashi, K. (2020). Why is the mahalanobis distance effective for anomaly detection? *arXiv preprint arXiv:2003.00402*.

Kingma, D. P. and Ba, J. (2015). Adam: A method for stochastic optimization. In Bengio, Y. and LeCun, Y., editors, *3rd International Conference on Learning Representations, ICLR 2015, San Diego, CA, USA, May 7-9, 2015, Conference Track Proceedings*.

Kirkpatrick, J., Pascanu, R., Rabinowitz, N., Veness, J., Desjardins, G., Rusu, A. A., Milan, K., Quan, J., Ramalho, T., Grabska-Barwinska, A., et al. (2017). Overcoming catastrophic forgetting in neural networks. *Proceedings of the national academy of sciences*, 114(13):3521–3526.

Kornblith, S., Shlens, J., and Le, Q. V. (2019). Do better imagenet models transfer better? In *Proceedings of the IEEE/CVF Conference on Computer Vision and Pattern Recognition*, pages 2661–2671.

Ledoit, O., Wolf, M., et al. (2004). A well-conditioned estimator for large-dimensional covariance matrices. *Journal of Multivariate Analysis*, 88(2):365–411.

Lee, K., Lee, K., Lee, H., and Shin, J. (2018). A simple unified framework for detecting out-of-distribution samples and adversarial attacks. In *Advances in Neural Information Processing Systems*, pages 7167–7177.

Li, C.-L., Sohn, K., Yoon, J., and Pfister, T. (2021). Cutpaste: Self-supervised learning for anomaly detection and localization. In *2021 IEEE/CVF Conference on Computer Vision and Pattern Recognition (CVPR)*, pages 9659–9669.

Li, H., Singh, B., Najibi, M., Wu, Z., and Davis, L. S. (2019). An analysis of pre-training on object detection. *arXiv preprint arXiv:1904.05871*.

Liu, W., Li, R., Zheng, M., Karanam, S., Wu, Z., Bhanu, B., Radke, R. J., and Camps, O. (2020). Towards visually explaining variational autoencoders. In *Proceedings of the IEEE/CVF Conference on Computer Vision and Pattern Recognition (CVPR)*.

Liznerski, P., Ruff, L., Vandermeulen, R. A., Franks, B. J., Kloft, M., and Müller, K. R. (2021). Explainable deep one-class classification. In *International Conference on Learning Representations*.

Mahalanobis, P. C. (1936). On the generalized distance in statistics. National Institute of Science of India.

Naseer, M. M., Ranasinghe, K., Khan, S. H., Hayat, M., Shahbaz Khan, F., and Yang, M.-H. (2021). Intriguing properties of vision transformers. *Advances in Neural Information Processing Systems*, 34.

Perera, P. and Patel, V. M. (2019). Learning deep features for one-class classification. *IEEE Transactions on Image Processing*, 28(11):5450–5463.

Reiss, T., Cohen, N., Bergman, L., and Hoshen, Y. (2021). Panda: Adapting pretrained features for anomaly detection and segmentation. In *Proceedings of the IEEE/CVF Conference on Computer Vision and Pattern Recognition (CVPR)*, pages 2806–2814.

Rezende, D. and Mohamed, S. (2015). Variational inference with normalizing flows. In Bach, F. and Blei, D., editors, *Proceedings of the 32nd International Conference on Machine Learning*, volume 37 of *Proceedings of Machine Learning Research*, pages 1530–1538, Lille, France. PMLR.

Rippel, O., Haumering, P., Brauers, J., and Merhof, D. (2021a). Anomaly detection for the automated visual inspection of pet preform closures. In *2021 26th IEEE International Conference on Emerging Technologies and Factory Automation (ETFA)*, volume 1.

Rippel, O. and Merhof, D. (2021). Leveraging pre-trained segmentation networks for anomaly segmentation. In *2021 26th IEEE International Conference on Emerging Technologies and Factory Automation (ETFA)*, pages 01–04.

Rippel, O., Mertens, P., König, E., and Merhof, D. (2021b). Gaussian anomaly detection by modeling the distribution of normal data in pretrained deep features. *IEEE Transactions on Instrumentation and Measurement*, 70:1–13.

Rippel, O., Mertens, P., and Merhof, D. (2021c). Modeling the distribution of normal data in pre-trained deep features for anomaly detection. In *2020 25th International Conference on Pattern Recognition (ICPR)*, pages 6726–6733.

Rippel, O., Müller, M., Münkel, A., Gries, T., and Merhof, D. (2021d). Estimating the probability density function of new fabrics for fabric anomaly detection. In *10th International Conference on Pattern Recognition Applications and Methods (ICPRAM)*.

Rodríguez, P., Gonzàlez, J., Cucurull, G., Gonfaus, J. M., and Roca, F. X. (2017). Regularizing cnns with locally constrained decorrelations. In *5th International Conference on Learning Representations, ICLR 2017, Toulon, France, April 24-26, 2017, Conference Track Proceedings*. OpenReview.net.

Rudolph, M., Wandt, B., and Rosenhahn, B. (2021). Same same but differnet: Semi-supervised defect detection with normalizing flows. In *Winter Conference on Applications of Computer Vision (WACV)*.

Ruff, L., Kauffmann, J. R., Vandermeulen, R. A., Montavon, G., Samek, W., Kloft, M., Dietterich, T. G., and Müller, K. R. (2021). A unifying review of deep and shallow anomaly detection. *Proceedings of the IEEE*, pages 1–40.

Ruff, L., Vandermeulen, R., Goernitz, N., Deecke, L., Siddiqui, S. A., Binder, A., Müller, E., and Kloft, M. (2018). Deep one-class classification. In Dy, J. and Krause, A., editors, *Proceedings of the 35th International Conference on Machine Learning*, volume 80 of *Proceedings of Machine Learning Research*, pages 4393–4402, Stockholmsmässan, Stockholm Sweden. PMLR.

Ruff, L., Vandermeulen, R. A., Franks, B. J., Müller, K.-R., and Kloft, M. (2020). Rethinking assumptions in deep anomaly detection. *arXiv preprint arXiv:2006.00339*.

Sabokrou, M., Fayyaz, M., Fathy, M., Moayed, Z., and Klette, R. (2018). Deep-anomaly: Fully convolutional neural network for fast anomaly detection in crowded scenes. *Computer Vision and Image Understanding*, 172:88–97.

Schlegl, T., Seeböck, P., Waldstein, S. M., Langs, G., and Schmidt-Erfurth, U. (2019). f-AnoGAN: Fast unsupervised anomaly detection with generative adversarial networks. *Medical image analysis*, 54:30–44.

Schölkopf, B., Platt, J. C., Shawe-Taylor, J., Smola, A. J., and Williamson, R. C. (2001). Estimating the support of a high-dimensional distribution. *Neural computation*, 13(7):1443–1471.

Simonyan, K. and Zisserman, A. (2015). Very deep convolutional networks for large-scale image recognition. In Bengio, Y. and LeCun, Y., editors, *3rd International Conference on Learning Representations, ICLR 2015, San Diego, CA, USA, May 7-9, 2015, Conference Track Proceedings*.

Tan, M. and Le, Q. V. (2019). EfficientNet: Rethinking model scaling for convolutional neural networks. In Chaudhuri, K. and Salakhutdinov, R., editors, *Proceedings of the 36th International Conference on Machine Learning, ICML 2019, 9-15 June 2019, Long Beach, California, USA*, volume 97 of *Proceedings of Machine Learning Research*, pages 6105–6114. PMLR.

Tax, D. M. and Müller, K.-R. (2003). Feature extraction for one-class classification. In *Artificial Neural Networks and Neural Information Processing—ICANN/ICONIP 2003*, pages 342–349. Springer.

Tayeh, T., Aburakhia, S., Myers, R., and Shami, A. (2020). Distance-based anomaly detection for industrial surfaces using triplet networks. In *2020 11th IEEE Annual Information Technology, Electronics and Mobile Communication Conference (IEMCON)*, pages 0372–0377.

Vaswani, A., Shazeer, N., Parmar, N., Uszkoreit, J., Jones, L., Gomez, A. N., Kaiser, L. u., and Polosukhin, I. (2017). Attention is all you need. In Guyon, I., Luxburg, U. V., Bengio, S., Wallach, H., Fergus, R., Vishwanathan, S., and Garnett, R., editors, *Advances in Neural Information Processing Systems*, volume 30. Curran Associates, Inc.

Venkataramanan, S., Peng, K.-C., Singh, R. V., and Mahalanobis, A. (2020). Attention guided anomaly localization in images. In Vedaldi, A., Bischof, H., Brox, T., and Frahm, J.-M., editors, *Computer Vision – ECCV 2020*, pages 485–503, Cham. Springer International Publishing.

Ye, Z., Chen, Y., and Zheng, H. (2021). Understanding the effect of bias in deep anomaly detection. In Zhou, Z.-H., editor, *Proceedings of the Thirtieth International Joint Conference on Artificial Intelligence, IJCAI 2021, Virtual Event / Montreal, Canada, 19-27 August 2021*, pages 3314–3320. ijcai.org.

Yi, J. and Yoon, S. (2020). Patch svdd: Patch-level svdd for anomaly detection and segmentation. In *Proceedings of the Asian Conference on Computer Vision (ACCV)*.

Zavrtanik, V., Kristan, M., and Skčaj, D. (2020). Reconstruction by inpainting for visual anomaly detection. *Pattern Recognition*, page 107706.